PREVENTING REVERSE POWER FLOW BY OPTIMAL COORDINATION OF PV FEED-IN: A CASE STUDY IN SOUTHERN BRAZIL

André Ulrich[1], Vinícius Hirassaki[2], Sascha Birk[1], Helena F. Naspolini[2], Eduardo L. O. Batista[2], Ricardo Rüther[2], Thorsten Schneiders[1]

[1]University of Applied Sciences Cologne (Germany)

[2]Universidade Federal de Santa Catarina, Florianópolis (Brazil)

Abstract

System operators (SOs) in Brazil are experiencing growing times with reverse power flows at their sub-stations. These reverse power flows are due to increasing installations of photovoltaic (PV) systems, and may lead to technical complications. Therefore, SOs are looking for solutions to counter these reverse power flows. One approach is to curtail PV to zero feed-in for times with reverse power flows. This results in the loss of sustainable energy from PV for the Brazilian energy system. Alternatively, this paper presents an optimization model which limits the power flow for a feeder at the sub-station level, by coordinating a fair down-regulation of PV across the grid. PV estimate and prediction, based on machine learning, are used, to calculate the feeder's pure load and to predict times of reverse power flows. This approach enables the use of excess PV by nodes without PV generation, increasing the consumption of sustainable energy in the system while preventing reverse power flows at the SOs sub-station. Results show that the ANN models produced satisfying results, and were deemed adequate for the purposes of this study. Up to 3.2 MW of reverse power flow occurred during the considered time periods, resulting in 1071 MWh over all analyzed periods. If all distributed PV were to be curtailed, 2817 MWh of renewable energy would not be utilized, which represents approximately 46.6% of total PV generation considered in the feeder. Through the dispatch optimization, the curtailment would only affect 1071 MWh of PV energy, representing 17.7% of total PV generation in the feeder.

Keywords: power system, reverse power flow, photovoltaic, optimization, machine learning

1. Introduction

In the first bimester of 2025, Brazil's electricity mix included approximately 54,900 MW of photovoltaic (PV) capacity, of which an estimated 68% constituted Distributed Energy Resources (DER) (ABSOLAR, 2025). The accelerated expansion of distributed photovoltaic generation in Brazil has introduced a range of operational challenges to the electric power system. The reversal of power flow is one such challenge, and has recently been addressed through specific regulatory measures (ANEEL, 2023a). This phenomenon occurs when the aggregated generation from multiple PV DER units connected to the same feeder exceeds the local electricity demand, thereby inducing reverse power flow—from loads back to the substation—through distribution transformers and substations. Such reversals can give rise to technical complications, such as phase imbalance, elevated voltage levels, variations in power factor, among other adverse effects (ANEEL, 2023b). Neiva et al. study network protection false tripping in case of reverse power flows in a Brazilian grid. They conclude it to be difficult to differentiate these cases from actual failures, highlighting the demand for countermeasures (Neiva, 2021).

While certain measures could address this issue—such as energy storage technologies (De Oliviera, 2023) or grid reconfigurations—these solutions are not necessarily applicable to all cases within the Brazilian context (ANEEL, 2024). The use of energy storage in distribution networks is still in its early stages in the country and network reconfigurations are not always feasible. In some cases, new PV installations are instructed to operate in a grid-zero configuration in order to avoid power flow reversal (ANEEL, 2023a). In the work by Almeida et al., the limitation of active power feed-in, voltage regulation as well as reactive power feed-in from the customer side and the energy companies were analyzed regarding their capability to handle voltage rise due to excess DER generation. All four measures showed positive effects on voltages in the grid (Almeida, 2018).

Holguin et al. propose a methodology to identify reverse power flows and disconnect generation units, depending on the voltages at the surrounding nodes (Holguin, 2020). Overall, the literature shows a favour for curtailing PV in order to prevent negative effects due to excessive PV feed-in. A body of literature has emerged to curtail PV in a fair manner among the PV systems in the grid (Gebbran, 2021; Poudel, 2022). However, these works focus on voltage regulation, rather than avoiding reverse power flows, which are a possible cause of network protection false tripping.

10.18086/swc.2025.07.11 Available at http://proceedings.ises.org

In this paper, a potential solution to the issue of reverse power flow and connected network protection false tripping is explored. This solution is based on the optimal dispatch of distributed generation from each prosumer unit, aiming to compensate for other loads within the feeder, thereby resulting in a zero or positive power flow at the feeder substation. To achieve this, a machine learning model is employed to predict the occurrence of reverse power flows and an optimization model is used to calculate the optimal dispatch for each prosumer unit connected to the feeder.

2. Methodology

For a realistic model of a Brazilian grid, we use grid data from a real feeder located in the southern region of Brazil. For this purpose, we consider all switches connecting the considered feeder to other feeders as open. This allows for a consideration as a radial grid. Other switches connecting transformers and the remaining infrastructure to the feeder are considered to be closed, to capture all connected load and PV generators. All loads and generation connected to a transformer are aggregated.

Based on the grid topology as well as demand and generation profiles, we use an optimization model, to dispatch the feed-in of the individual PV plants in the considered grid. This dispatch is calculated in a manner, so that there is no reverse power flow through the main station – all the generated energy is to be used in the feeder. If generation exceeds demand in the feeder, the PV feed-in needs to be regulated down. This down-regulation is to happen in a fair manner, so that all the PV plants get regulated down approximately the same relative amount. The described methodology is depicted in Fig. 1.

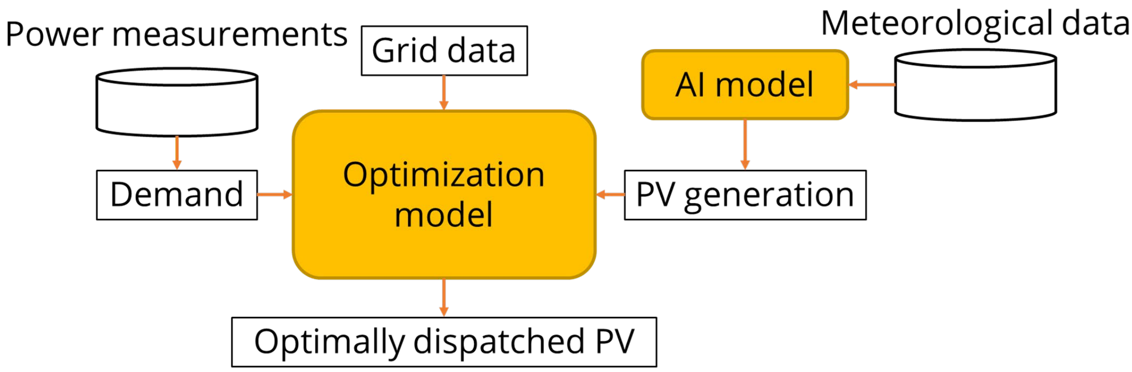

Fig. 1 Schematic deception of the procedure for optimal PV dispatch

2.1 Grid Data Preprocessing

In order to provide a realistic setting for the developed algorithm, this work is based on real grid data from a grid operator in southern Brazil. The grid suffers from reverse power flows over the main transformer at the point of common coupling. The algorithm, developed in this work, is suited for optimizing PV generation in a radial grid. Therefore, all PV generation is aggregated at the transformers, connecting them to the main line, as depicted in Fig. 2. The resulting grid topology is a string with 25 buses. The total number of PV systems in the grid is 257, and the total installed PV power is 3563.49 kWp, which was divided between the 25 buses proportionally to the aggregated transformer power in each bus. The aggregated installed capacity of transformers behind each node on the main grid line is given in Table 3 in the appendix.

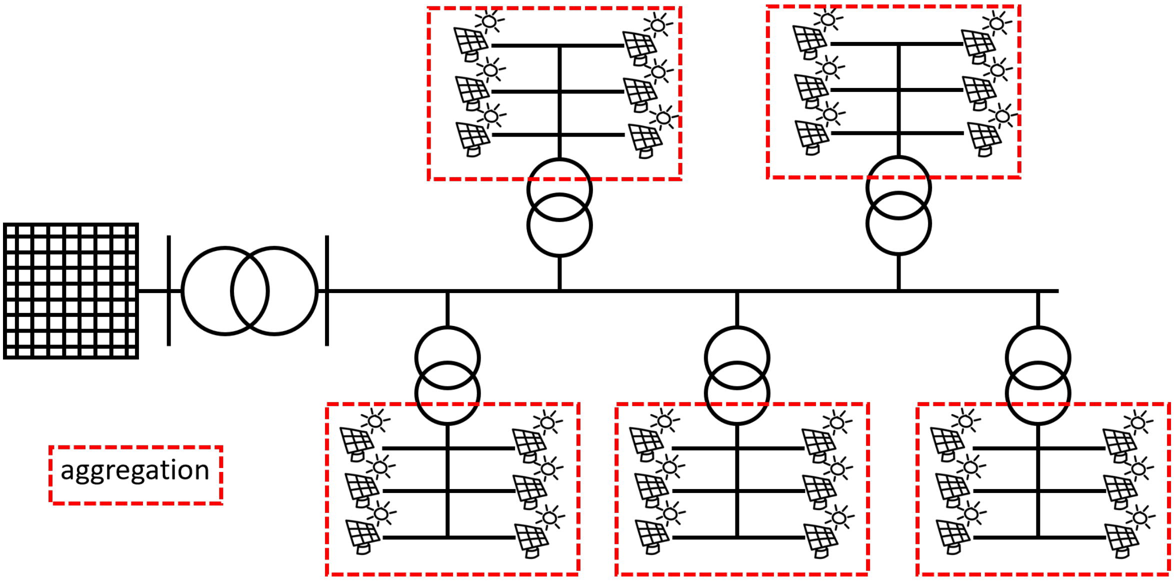

Fig. 2 Schematic aggregation of PV systems in the meshed grid topology

2.2 Power Measurement Data Preprocessing

For the grid described above, hourly power measurement data at the point of common coupling was provided by the system operator from 1st of April 2024 until 1st of April 2025. From these measurements, an estimate of the PV generation (Section 2.3) is subtracted to receive the estimated demand profile for the grid. This step is necessary, as the real PV generation profiles are not available.

Given that this paper focuses on reverse power flow instances caused by PV generation, the analysis is limited to daytime hours only. For this purpose, the apparent solar elevation was calculated for each hour in the analyzed period for the location of the feeder, and any data point with an apparent elevation lower than 5° was discarded. In this manner, the solar resource's inherent seasonality in tropical locations was accounted for, and the analysis period was guaranteed to be limited to daytime hours for all 12 months of the year.

The resulting demand profile is checked for any remaining negative power flows, and the respective time periods are excluded from the optimization. This step is necessary, since there currently is no way to measure the PV generation of all distributed systems within the feeder and, consequently, an estimate had to be used, which could lead to some errors. The total demand profile is then distributed among the 25 transformers in the grid, according to the ratio of the transformer's rated power to the total installed transformer power within the grid. This results in one demand profile per node in the simplified grid model (Section 2.1). This way, the total demand is proportionally distributed among the individual transformers. The demand profiles are then fed into the optimization model (Section 2.4).

2.3 Machine Learning Model for PV generation estimation and prediction

Artificial Neural Network (ANN) models were developed to estimate and predict photovoltaic energy generation one hour ahead based on meteorological data. These models' architectures were based on the works of Hirassaki (2024), which developed an ANN model to estimate the PV generation from aggregated DERs in Florianópolis (Santa Catarina, Brazil), a city located in southern Brazil. The models consisted of two hidden layers: the first layer had 500 neurons, and the second had 200 neurons. The models were trained using meteorological data and timestamps as the input attributes and aggregated PV Capacity Factor (CF) as the target variable. Fig. 3 shows a representative example of an ANN.

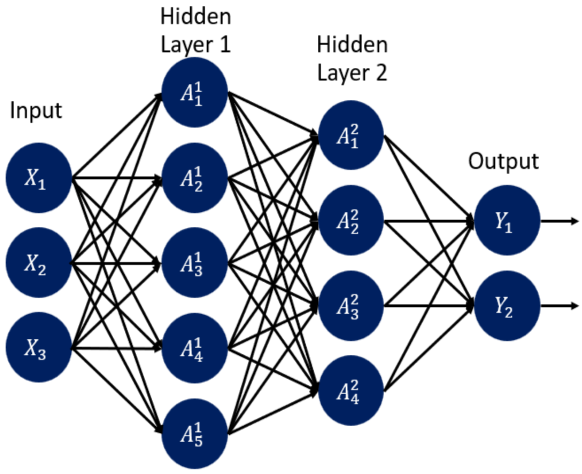

Fig. 3 Representative example of an ANN

Meteorological data used include solar irradiance, maximum and minimum air temperature, maximum and minimum relative humidity, maximum and minimum atmospheric pressure, wind speed, and wind gust (Hirassaki, 2024). These measurements were obtained from the Brazilian National Institute of Meteorology (INMET, 2025), which has several meteorological stations spread throughout Brazil and provides the measurements from each station in an hourly basis on their official website. Data from 2019 from three meteorological stations (one close to the analyzed feeder and two from neighboring cities) was collected for the purposes of training the ANN models, whereas data from 1st of April 2024 until 1st of April 2025 was collected to estimate and predict the PV generation on the feeder.

In addition to the meteorological data, timestamps were also used as input to the ANN models. However, to better represent the seasonality of the solar resource and improve the models' performance, the apparent solar elevation and the cosine of the solar azimuth were used as inputs instead, calculated utilizing the pvlib library (Anderson et. al., 2023) and the location of each meteorological station. The cosine of the solar azimuth was used because it correlates better to the solar resource than the azimuth itself.

The aggregated PV CF was calculated from measurements of several distributed residential PV systems installed in the same region as the studied feeder. This data was provided by the distribution company and is comprised of PV generated power measured in 5-minute intervals, for the entire year of 2019. This data was filtered using a method based on the works of Antoniolli et al. (2022) to eliminate faulty systems and systems with excessive measurement errors: for each system, it was evaluated whether it had, for all 12 months of the year, at least 15 days with a minimum of 8 hours of PV generation greater than 50W; and the systems that met those conditions were subsequently filtered for outliers using a recursive interquartile range filter. The CF was then calculated for each system, and the average CF of all filtered systems within 50 km of each meteorological station was calculated to represent the generation profile of distributed PV systems in this area, in the form of a virtual power plant.

Finally, the ANN models were trained using the meteorological and aggregated PV CF data from 2019. The models were trained using data from two neighboring cities and tested using data from the city where the feeder is located, with the purpose of evaluating their accuracy. Meteorological data from 1st of April 2024 until 1st of April 2025 was then inputted in the trained models to generate an estimate and a one-hour-ahead prediction of the PV generation in the studied feeder. The key difference between the estimation and prediction ANN models lies in the synchronization between meteorological data and PV CF data: the estimation model utilizes data from the same timestamp to estimate PV generation, whereas the prediction model utilizes data from one hour prior to predict PV generation.

2.4 Optimization model for optimized PV dispatch

The optimization model is based on several inputs like predicted demands, PV feed-in and grid topology, as depicted in Fig. 1. The goal of the optimization is to allow as much PV feed-in as possible, while ensuring at the same time no reverse power flow will occur. Therefore, the amount of down-regulation of PV feed-in (per PV plant, per time step) is considered as a decision variable. Furthermore, the optimization model implements several constraints that will ensure to prevent reverse power flow and to also ensure a fair distribution of down-regulation among all the PV plants in the considered grid. The optimization model is taken from (Ulrich et al., 2023), where it was used to coordinate EV charging. Here, the optimization model is adapted to coordinate PV feed-in instead of EV charging. The rest of this section will detail all considered sets, decision variables, parameters, constraints and the objective.

As sets we consider the set T of all time steps, the set N of all nodes on the considered grid line, the set $N_{PV} \subseteq N$ of all nodes with a PV plant attached and the set $L$of all line segments between the nodes.

Parameters are predicted demands $P_{dem} \in \mathbb{R}_{+}^{T \times N_{PV}}$ and predicted PV feed-in $P_{PV} \in \mathbb{R}_{+}^{T \times N_{PV}}$per node and timestep, voltages $U \in \mathbb{R}_{+}^{N}$ at the individual nodes and Impedances $Z \in \mathbb{R}_{+}^{L}$ of the individual lines between the nodes.

The decision variable is the share of realized PV feed-in after down-regulation $a \in [0,\ 1]^{T \times N_{PV}}$ for each PV plant at each time step, such that the realized PV feed-in $P_{t,n}^{PV,r}$ after down-regulation can be calculated as $P_{t,n}^{PV,r} = a_{t,n} P_{t,n}^{PV}$.

The objective function aims at maximizing the realized PV feed-in for each node at each time step. This is formulated according to equation (1):

$$\max. \sum_{n,t \in \mathcal{N}_{\mathrm{PV}} \times \mathcal{T}} a_{n,t} \tag{1}$$

Constraints ensure the grid is not overloaded at any time steps, and a proportionally fair amount of down-regulation is distributed among the PV plants. The constraint in equation (2) ensures the voltage at the last node does not drop below a permissible voltage V_{min}, where V_0 is voltage at the main station transformer low-voltage side, Z_l is the impedance of the l-th line.

$$V_0 - \sum_{l \in \mathcal{L}} \left(Z_l \sum_{\substack{n \in \mathcal{N} \\ n \geq l}} \left(I_{n,t}^{\mathrm{dem}} - a_{n,t} I_{n,t}^{\mathrm{PV}} \right) \right) \geq V_{\min} \quad \forall t \in \mathcal{T} \tag{2}$$

The constraint in equation (3) ensures that there is no reverse power flow through the transformer:

$$\sum_{n \in \mathcal{N}} \left(\left(I_{n,t}^{\mathrm{dem}} - a_{n,t} I_{n,t}^{\mathrm{PV}} \right) V_n \right) \geq 0 \quad \forall t \in \mathcal{T} \tag{3}$$

The constraint in equation (4) ensures that none of the lines connecting the nodes is overloaded:

$$\sum_{\substack{n \in \mathcal{N} \\ n \geq l}} \left(I_{n,t}^{\mathrm{dem}} - a_{n,t} I_{n,t}^{\mathrm{PV}} \right) \leq I_l^{\max} \quad \forall l, t \in \mathcal{L} \times \mathcal{T} \tag{4}$$

Finally, the constraint in equation (5) ensures that the amount of down-regulated PV feed-in is equally distributed among all the PV plants connected to the considered grid line:

$$\sum_{t \in \mathcal{T}} a_{n,t} - \sum_{t \in \mathcal{T}} a_{m,t} \leq \Delta a_{\max} \quad \forall n, m \in \mathcal{N}^2 \text{ with } n > m \tag{5}$$

The described optimization model, however, is only valid for strictly radial grids. Therefore, transformers and PV stations behind the nodes of the main line are aggregated at each node (as described in section 2.1). A model of a simplified grid line with all the relevant quantities for the optimization is given in Fig. 4.

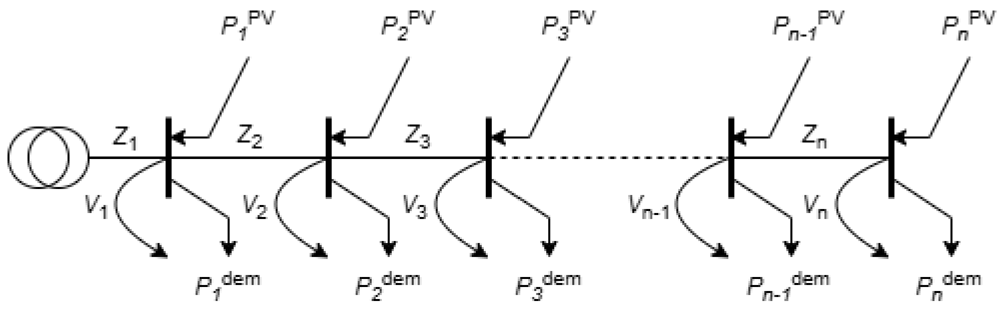

Fig. 4 Example for a simplified grid line with all the quantities relevant for the optimization model

The optimization model is formulated using the Python framework pyomo (Bynum et al., 2021) and solved using GLPK (GLPK, 2025). The resulting optimized PV feed-in as well as given demand data are then fed into a pandapower (Thurner et al., 2018) power flow simulation. This way the results of optimized PV feed-in are validated by checking for any occurrences of reverse power flows.

3. Results

3.1 PV generation estimate and prediction

Table 1shows the R^2 score, Root Mean Square Error (RMSE) and Mean Absolute Error (MAE) for the PV generation estimate and prediction ANN models.

Table 1 Test results for the PV generation estimate and prediction models

Model	R^2	RMSE	MAE
Estimate	94.66%	5.28%	3.76%
Prediction	87.45%	8.11 %	6.01%

The table shows that the estimate model had a higher accuracy than the prediction model in all three metrics. However, both models demonstrated acceptable results, with low error metrics and high correlation scores. As such, both models could be adequately used to estimate and predict the PV generation for the purposes of this study.

3.2 Power Measurement Data Preprocessing

After the demand measurements provided by the system operator were corrected using the PV generation estimate, 107 instances of reverse power flow remained, spread throughout 32 days. Table 2 shows the days which still present reverse power flow instances.

Table 2 Days with reverse power flow instances after PV correction

Month	May	Jun	Jul	Aug	Sep	Oct	Nov	Dec	Jan	Feb	Mar
Days	04, 05, 12, 19, 26	01, 02, 23, 30	20, 21, 28, 30	11, 25	22	13, 17, 20, 27	03, 09, 29, 03	04, 07, 08, 15, 25	26	23	28

Given that the number of days was not significant, and that each month only had an unsubstantial fraction of days with reverse power flow, those days were not considered for the dispatch optimization.

3.3 Optimized PV feed-in

We investigate the grid as described in Section 2.1. Demand as well as installed PV capacity are aggregated behind the transformers attached to the middle voltage feeder. This way, the whole considered grid can be depicted as a radial grid. The PV feed-in in this radial grid is then optimized using the algorithm described in section 2.4. The aggregated installed capacity of transformers behind each node on the main grid line is given in Table 3 in the appendix. Using a given demand and predicted PV feed-in (as described in section 2.3), the optimization algorithm determines an optimal down-regulation policy. This down regulation happens in such a way that no PV system is discriminated against, and no reverse power flows occur.

The revised overall demand data (see section 2.2) as well as predicted PV feed-in are depicted in Fig. 5.

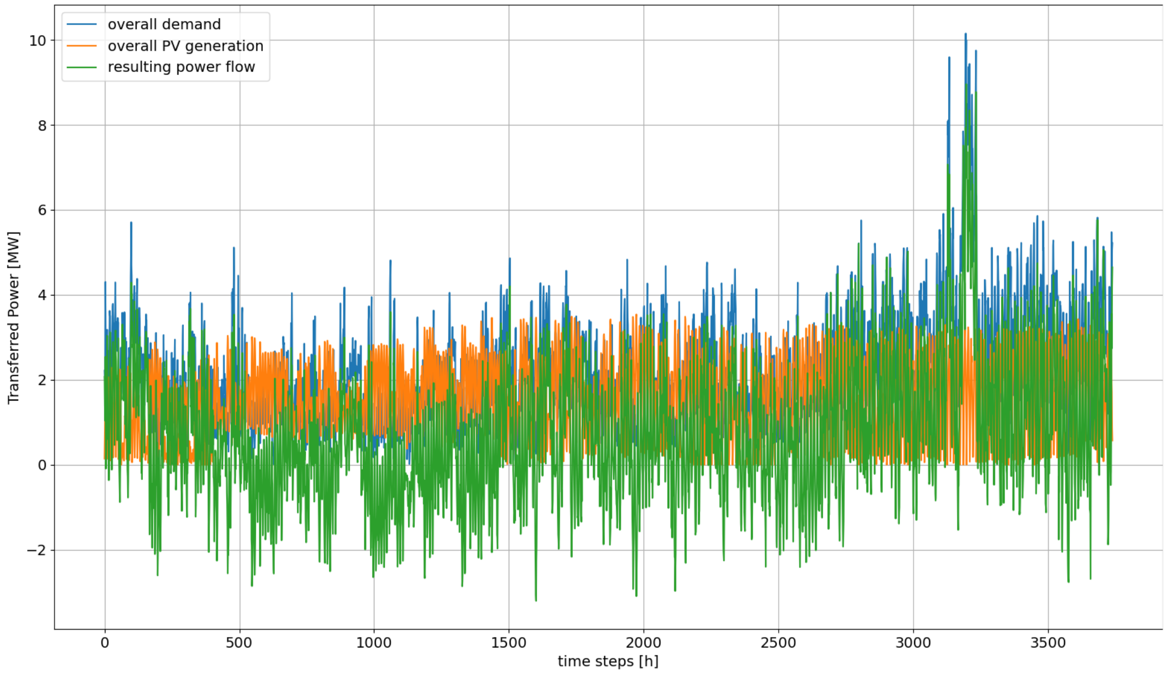

Fig. 5 Revised overall demand (blue line), predicted overall PV generation (orange line) and resulting power flow through the main station (green line). There are many reverse power flows occuring during the considered time horizon of up to –3.2 MW.

This already shows reverse power flows of up to –3.2 MW occurring during the considered time horizon, depicted by the green line. If the PV feed-in is realized as predicted (the orange line), without any down regulation, this will lead to a total amount of 1071 MWh of electrical energy, flowing through the main station in reverse, over the course of 1229 hours during the considered time horizon. Following the official operation strategy in case of reverse power flow (curtail all the PV feed-in to zero), this would mean that 2817 MWh renewable energy is curtailed. In relation to the total of 6042 MWh predicted PV feed-in during the considered time horizon, this means that 46.6 % of PV feed-in cannot be utilized.

However, if the PV feed-in is only curtailed to the point where there is no more reverse power flow (instead of complete curtailment to zero), then only 1071 MWh of PV feed-in cannot be utilized due to the curtailment. This equals 17.7 % of the predicted PV feed-in. The constraint in equation (5) allows the optimization to shift the down-regulation among PV systems. It only requires the relative down-regulation to be the same among all PV systems when considering the complete time horizon. So if – for whatever reason – it is beneficial for grid operation to power down one specific PV system but keep another PV system running, then the optimization has the freedom to do this. However, in the end, all the PV systems will experience the same relative amount of down-regulation. An example for this optimally coordinated down-regulation of PV systems for an exemplary week, is given in Fig. 6. The figure shows 25 lines on each of the three plots: one line for all aggregated PV systems behind one node. The red line represents the feed-in of an especially large PV system (according to the distributed aggregated transformer power, see section 2.1)

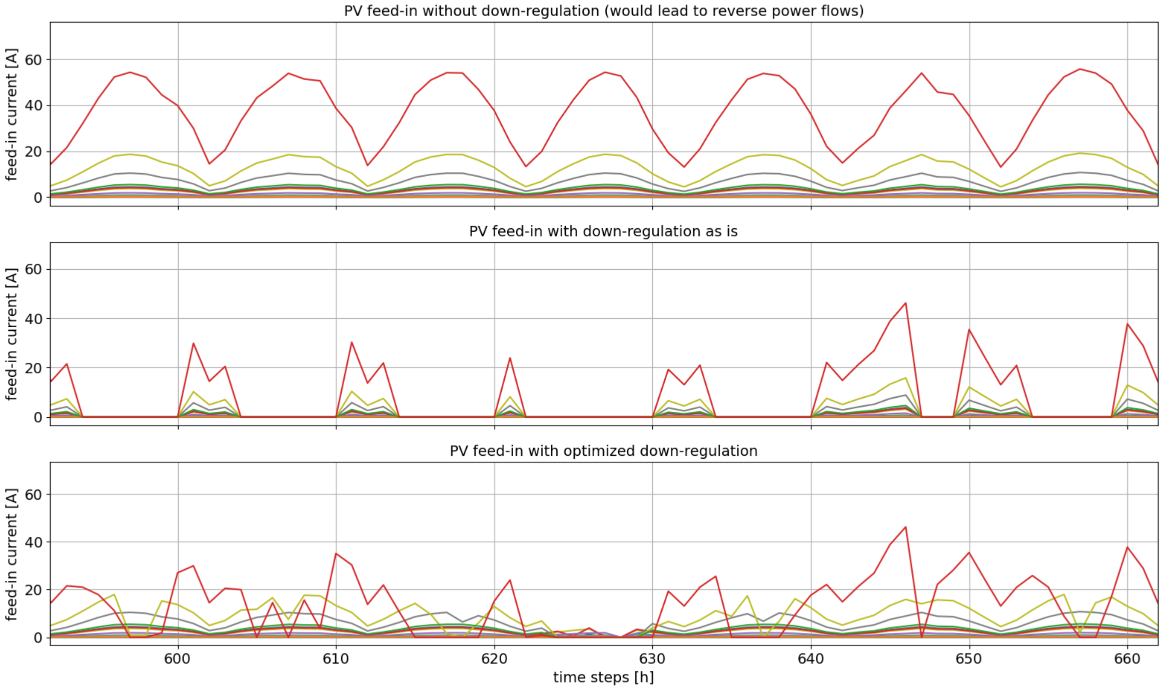

Fig. 6 One exemplary week of PV feed-in. The upper graph shows the PV feed-in without any down-regulation, the middle graph shows the PV feed-in with down-regulation according to the Brazilian SOs policy, and the lower graph shows the PV feed-in with optimized down-regulation.

When inspecting this figure, it should be kept in mind that the night-times were filtered out of the data (see section 2.2) which is the reason why the PV peaks directly follow next to each other, without the typical "night valley". For example, on the third day of the week under consideration, mainly the two largest PV systems are curtailed. On the fourth day, however, almost all PV systems are curtailed, at least for a short time. This example shows the freedom of the optimization to curtail whichever PV system seems most beneficial for grid operation.

The resulting power flow through the main station transformer in case of optimized and unoptimized PV feed-in is shown in Fig. 7.

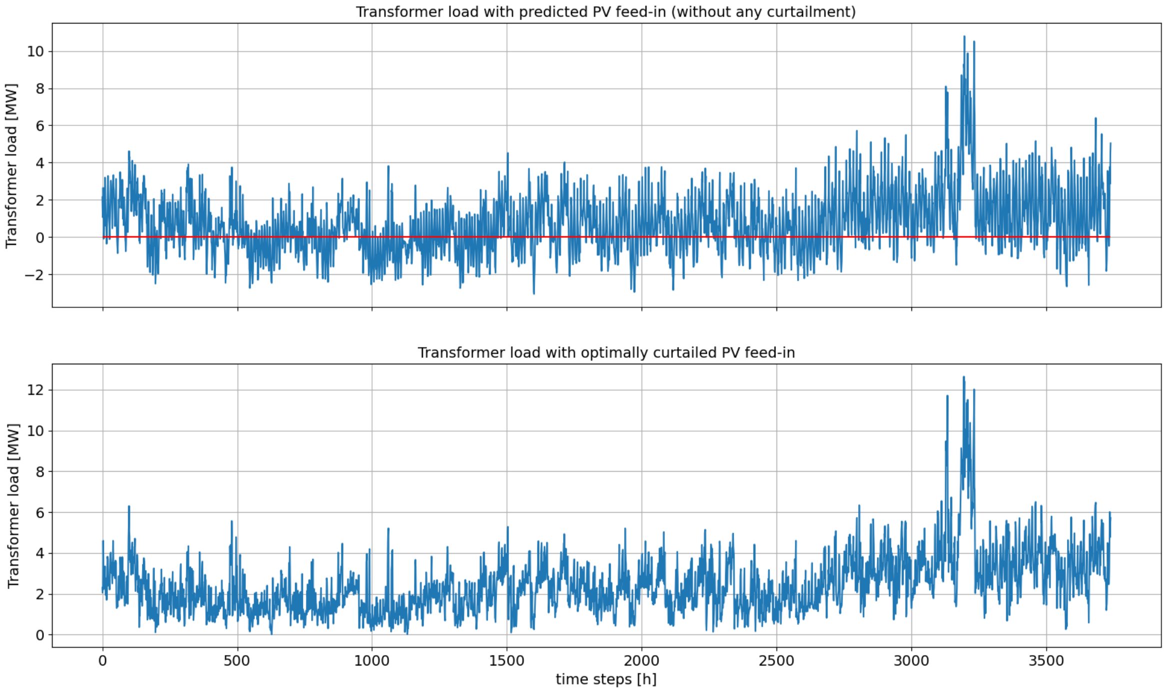

Fig. 7 Resulting power flow through the main station transformer in case of unoptimized (upper graph) and optimized (lower graph) PV feed-in.

In the case of optimized PV feed-in, there are no more reverse power flows to be observed. The power flow through the main station never drops below zero.

4. Conclusion

The proposed methodology prevents reverse power flows in system operators sub-stations due to excessive PV feed-in. Using an ANN, the PV generation can be predicted for the upcoming horizon using meteorological data from a nearby station. The optimization model dispatches the PV feed-in to curtail excess generation to the point where no reverse power flows occur at the sub-station. This approach enables more PV consumption within the grid, compared to previous approaches, as it does not limit the individual PV feed-in to zero. Therefore, a fair distribution of down-regulation among the PV plants can be realized, limiting discrimination against individual PV systems. The ANN models produced satisfying results, and while the estimate model proved to be more accurate than the prediction model, both were deemed adequate for the purposes of this study. Measured data of the feeder reveals that up to 3.2 MW of reverse power flow occurred during the considered time periods, resulting in 1071 MWh over the entire analyzed periods. If all distributed PV were to be curtailed, 2817 MWh of renewable energy would not be utilized, which represents approximately 46.6% of total PV generation considered in the feeder. Through the dispatch optimization, the curtailment would only affect 1071 MWh of PV energy, representing 17.7% of total PV generation in the feeder. Due to the lack of distributed PV generation measurements in Brazilian distribution grids, an estimate had to be used to calculate the load in the feeder, which led to some remaining instances of reverse power flow that had to be eliminated from the analysis. Additionally, although the data provided by the DSO demonstrated that the majority of DERs in the feeder were PV generators, it is possible that some changes to the installed capacity were not reported to the DSO and, therefore, were not accounted for in this study, which could have also led to some errors. This work highlights the necessity of further studies on the management of DERs, especially in distribution feeders with high installed capacity of intermittent sources. As such, the inclusion of different DERs, such as wind power, should be considered for future works.

5. Acknowledgments

ECS4DRES is supported by the Chips Joint Undertaking under grant agreement number 101139790 and its members, including the top-up funding by Germany, Italy, Slovakia, Spain and The Netherlands.
Research work carried out within the scope of the activities of the National Institute for Technological Development of Photovoltaic Solar Energy Applications, INCT-DAESF, CNPq/MCTI/Brazil, Grant Number 408486/2024-4.
This research was supported by the Fundação de Amparo à Pesquisa e Inovação do Estado de Santa Catarina (FAPESC).

6. References

ABSOLAR, 2025. Panorama da solar fotovoltaica no Brasil e no mundo. https://www.absolar.org.br/mercado/infografico/. Access in 04/28/2025

ALMEIDA, G.L.S. and JOTA, P.R.S. A study of voltage rise in distribution grids with high concentration of power generators. Renewable Energy and Power Quality Journal, 2018, 1. Jg., S. 137-141.

ANDERSON, K., HANSEN, C., HOLMGREN, W., JENSEN, A., MIKOFSKI, M., and DRIESSE, A. “pvlib python: 2023 project update.” Journal of Open Source Software, 8(92), 5994, (2023). DOI: 10.21105/joss.05994.

ANEEL, 2023a. RESOLUÇÃO NORMATIVA ANEEL Nº 1.059, DE 7 DE FEVEREIRO DE 2023. 02/07/2023.

ANEEL, 2023b. Nota Técnica nº 76/2023-STD/STR/ANEEL. 08/31/2023. pp 19

ANEEL, 2024. Apresentação de Estudos de Inversão de Fluxo. Art. 73, §1º da REN nº 1.000/2021. 31/07/2024.

ANTONIOLLI, A.F. G.; MONTENEGRO, A.A.; ZOMER, C.D.; RÜTHER, R. AVALIAÇÃO TÉCNICA E ECONÔMICA ENTRE SISTEMAS FOTOVOLTAICOS APLICADOS A EDIFICAÇÕES (BAPV) E SISTEMAS IDEALMENTE INSTALADOS PARA MÁXIMA GERAÇÃO ANUALVI Congresso Brasileiro de Energia Solar. Anais...Belo Horizonte: 13/12/2016

BYNUM, M L.; HACKEBEIL, G.A.; HART, W E.; LAIRD, C.D.; NICHOLSON, B L.; SIIROLA, J.D; WATSON, Jean-Paul; WOODRUFF, David L. Pyomo - Optimization Modeling in Python, 3rd Edition. Springer, 2021

DE OLIVEIRA G.G., DARUI, C.B.F, DA CRUZ, M.S., FIGUEIRÓ, I.C, ROQUE, A.S., DE MELLO, R.M., DA VEIGA, M.F., DOS SANTOS, A.V. "Armazenamento Controlado de Energia para Redução de Impactos da Geração Fotovoltaica em Redes de Baixa Tensão," 2023 XV Brazilian Conference on Quality of Power (CBQEE), São Luiz, Brazil, 2023, pp. 1-6, doi: 10.1109/CBQEE59548.2023.10503600

GEBBRAN, D., MHANNA, S., MA, Y., CHAPMAN, A.C and VERBIC, G. Fair coordination of distributed energy resources with Volt-Var control and PV curtailment. Applied Energy, 2021, 286. Jg., S. 116546. doi: 10.1016/j.apenergy.2021.116546

GLPK, GNU Linear Programming Kit (2025), Version 5.0, http://gnu.org/software/glpk/glpk.html

HIRASSAKI, Vinícius. (2024). Usinas virtuais equivalentes representativas de múltiplos sistemas fotovoltaicos distribuídos em Florianópolis. [Master's thesis. Universidade Federal de Santa Catarina]. Repositório Institucional UFSC. https://repositorio.ufsc.br/handle/123456789/263689

HOLGUIN, J.P.; RODRIGUEZ, D.C.; RAMOS, G. Reverse power flow (RPF) detection and impact on protection coordination of distribution systems. IEEE Transactions on Industry Applications, 2020, 56. Jg., Nr. 3, S. 2393-2401.

INMET, 2025. Instituto Nacional de Meteorologia, Ministério de Agricultura e Pecuária, https://portal.inmet.gov.br/. Access 04/23/2025

NEIVA, L.J.R.; COELHO, F.C.R.; PERES, W. , FLAVIO, S.A., DIAS, L.R. Analysis of Power Flow Reversion in Distribution Transformers Due to Medium-Voltage Fault and Distributed Generation in Secondary Networks. J Control Autom Electr Syst 32, 1718–1727 (2021). https://doi.org/10.1007/s40313-021-00763-4

POUDEL, Shiva; MUKHERJEE, Monish; REIMAN, Andrew P. A fairness-based distributed energy coordination for voltage regulation in distribution systems. In: 2022 IEEE Green Technologies Conference (GreenTech). IEEE, 2022. S. 45-50.

THURNER, Leon; SCHEIDLER, Alexander; SCHÄFER, Florian; MENKE, Jan-Hendrik; DOLLICHON, Julian; MEIER, Friederike; MEINECKEN, Steffen; BRAUN, Martin. Pandapower – an Open Source Python Tool for Convenient Modelling, Analysis and Optimization of Electric Power Systems. In: 2018 IEEE Transactions on Power Systems, 2018, Jg. 33, Nr. 6, S. 6510-6521, doi: https://doi.org/10.1109/TPWRS.2018.2829021

ULRICH, André; BAUM Sergej; STADLER, Ingo; HOTZ, Christian; WAFFENSCHMIDT, Eberhard. Maximising Distribution Grid Utilisation by Optimising E-Car Charging Using Smart Meter Gateway Data. Energies, 2023, 16. Jg. doi: https://doi.org/10.3390/en16093790

Appendix

Table 3 Aggregated rated transformer power at each bus

Bus	Transformer (kW)
1	45
2	112.5
3	45
4	150
5	170
6	192.5
7	75
8	75
9	1150
10	45
11	1382.5
12	75
13	277.5
14	1285
15	582.5
16	75
17	150
18	3212.5
19	5712.5
20	45
21	10
22	45
23	1672.5
24	16555
25	30